

also examined, with the results depicted in Fig. 1, where total velocity increment is plotted against fraction of total available heat going to the hydrogen. As may be seen, this procedure can result in significant increases from the velocity increments found for either working fluid alone, with a maximum velocity increment of nearly 4000 m/s being achieved when approximately two-thirds of the heat is extracted by hydrogen.

Finally, one degree of realism was imposed with calculations using initial conditions for the working fluids as liquid hydrogen at 20 K and liquid nitrogen at 90 K. This required straightforward modification of the calculation of working fluid/capacitor mass ratios with the use of modified initial temperatures in Eq. (3) and the inclusion of an additional term in that equation to account for the heat of vaporization of the working fluids. Under these conditions, the maximum velocity increment attained was reduced to 2650 m/s, with the optimum nitrogen/hydrogen split being approximately 45/55. Obviously, further calculations using more realistic working fluid initial conditions, including inert masses for tankage and useful payload weights must be performed if one is to pursue this enthalpy rocket approach further.

### References

- <sup>1</sup>Parker, T. W., and Humble, R. W., "Theoretical Upper Limits on Enthalpy Rocket Performance," *Journal of Propulsion and Power*, Vol. 12, No. 2, 1996, pp. 445–448.
- <sup>2</sup>Gany, A., "Comment on 'Theoretical Upper Limits on Enthalpy Rocket Performance,'" *Journal of Propulsion and Power*, Vol. 13, No. 1, 1997, pp. 167, 168.

## Effects of Kinetic Rate Uncertainty on the Predicted Performance of Solar Thermal Rockets

D. Brian Landrum\* and Robert M. Beard†  
University of Alabama in Huntsville,  
Huntsville, Alabama 35899

### Introduction

SOLAR thermal propulsion has emerged as a candidate for future orbital transfer vehicles. In a solar thermal rocket, reflectors concentrate solar energy into an absorber that heats the propellant. Because of hydrogen's low molecular weight, a hydrogen-fueled solar thermal rocket operating at typical absorber temperatures of 2220–3390 K (4000–6100°R) can theoretically produce specific impulses  $I_{sp}$  of 700–1200 s. Previous research indicates that the actual  $I_{sp}$  delivered by solar thermal rockets is significantly lower than the predicted ideal value.<sup>1</sup> Therefore, accurate predictions of nonideal nozzle performance are essential to the development of these low-thrust systems.

Presented as Paper 96-2856 at the AIAA/ASME/SAE/ASEE 32nd Joint Propulsion Conference, Lake Buena Vista, FL, July 1–3, 1996; received May 5, 1997; revision received July 16, 1997; accepted for publication Aug. 2, 1997. Copyright © 1997 by the American Institute of Aeronautics and Astronautics, Inc. All rights reserved.

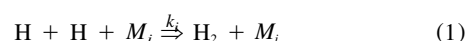
\*Assistant Professor, Propulsion Research Center, Department of Mechanical and Aerospace Engineering, RI E-33. Senior Member AIAA.

†Graduate Research Assistant, Propulsion Research Center, Department of Mechanical and Aerospace Engineering, RI E-32. Student Member AIAA.

Specific impulse losses are caused by flow divergence, viscous losses, and finite rate chemical kinetics.<sup>2</sup> As the hydrogen is heated in the absorber, the thermal energy input causes a fraction of the gas molecules to dissociate. The short residence time of the expanding gas in the small nozzle does not permit full chemical equilibrium to be reached. The magnitude of nonequilibrium is determined by the hydrogen recombination rate, which is a function of the chamber temperature and pressure, the divergent nozzle geometry, and the rate constant. A research literature review revealed hydrogen recombination rate constant variations of as much as two orders of magnitude.<sup>3,4</sup> Depending on the chamber conditions and the particular rate model chosen, this uncertainty could have a significant impact on solar thermal rocket performance predictions. The results of this study are applicable to the design of small-scale thrusters that use hot hydrogen propellant.

### Hydrogen Kinetics

The exothermic recombination of hydrogen is governed by two reactions



where  $M_i$  is either an atomic H or molecular  $H_2$  third-body. The rate constant of each reaction can be written in the Arrhenius form

$$k_i = A_i T^{N_i} \cdot \exp(-E_{ai}/RT) \quad (2)$$

A broad range of experimentally and analytically determined values for  $k_{H_2}$  and  $k_H$  are presented in the research literature.<sup>3–7</sup> Wetzel and Solomon<sup>4</sup> studied the impact of rate uncertainty on the performance of high-thrust (~44.5 kN or 10,000 lbf) nuclear thermal rockets, and defined a set of high, nominal, and low rates. The Warnatz recommended rate set was chosen for NASP propulsion technology research.<sup>5</sup> Baulch et al.<sup>6</sup> recommended a set of widely used rates. Cohen and Westberg<sup>7</sup> also defined a set of high, nominal, and low rates. The various rate constants are presented graphically vs temperature in Figs. 1 and 2. Also shown are hydrogen recombination rates used in the NASA-developed, finite difference Navier–Stokes (FDNS) code<sup>8</sup> and the two-dimensional kinetics (TDK) code.<sup>9</sup> In the temperature range of interest in the present study, the rate constant values vary by as much as two orders of magnitude.

### Numerical Model

The numerical simulations were performed with the CFD-ACE™ code.<sup>10</sup> The code uses a finite volume, pressure-based method to solve the Favre-averaged Navier–Stokes equations as a system of scalar transport equations in strongly conservative form

$$\frac{\partial \rho_\phi}{\partial t} + \frac{\partial}{\partial x_\beta} (\rho u_\beta \phi) = \frac{\partial}{\partial x_\beta} \left( \Gamma_\phi \frac{\partial \phi}{\partial x_\beta} \right) + S_\phi \quad (3)$$

where  $\rho$  is the density,  $u_\beta$  are the velocity components,  $\Gamma_\phi$  is the effective diffusion coefficient, and  $S_\phi$  is the scalar source term. An underrelaxed, implicit iterative procedure is used to solve steady-state problems. A hybrid, central-upwind scheme is used for the spatial differencing to model mixed subsonic/supersonic flow regimes typical of rocket nozzles. A SIMPLEC algorithm was chosen for the pressure-velocity coupling. Equilibrium, finite rate, and frozen chemistry can be modeled. The second author developed a postprocessing program that integrates the calculated properties across the nozzle exit to determine thrust, mass flow rate, and  $I_{sp}$ .

The nozzle had a 1.58 mm (0.06215 in.) throat radius, a divergent area ratio of 100:1, a convergent area ratio of 35:1,

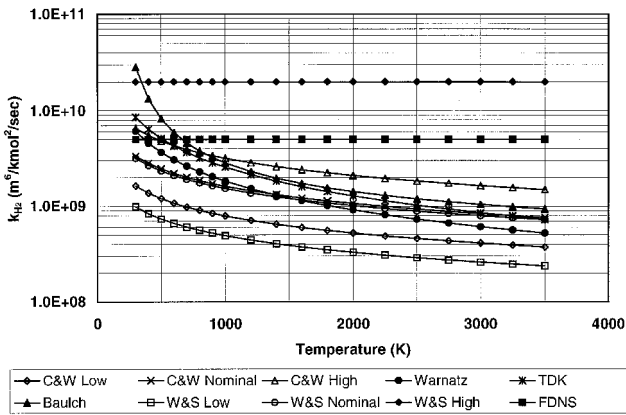


Fig. 1 Survey of hydrogen recombination rate constants for an  $H_2$  third body.

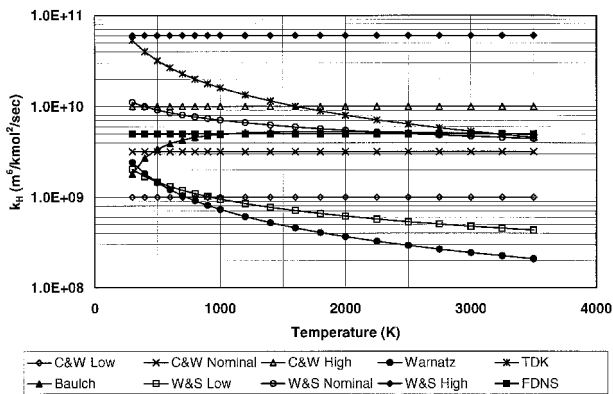


Fig. 2 Survey of hydrogen recombination rate constants for an  $H$  third body.

and was 57.91 mm (2.28 in.) long. The bell-shaped divergent nozzle contour was defined by a skewed parabola based on the throat radius, exit area ratio, exit angle ( $\theta_e \approx 9$  deg), and throat divergence angle ( $\theta_d \approx 32$  deg). Exponential stretching was employed to cluster the  $171 \times 71$  grid in the throat and near the nozzle wall where the highest flowfield gradients occur.

The inflow total pressure and total enthalpy were held constant at the nozzle inlet. The inflow radial velocity was assumed to be zero and the axial velocity was obtained by extrapolation from the interior. The inflow static temperature, pressure, and density were calculated using the constant total enthalpy isentropic relations and the perfect gas equation of state. All dependent variables were extrapolated from the interior at the predominantly supersonic exit. An adiabatic, no-slip velocity condition was assumed on the nozzle wall. Because of the significant viscous effects in these small nozzles, laminar flow was assumed.

## Results

A plenum chamber pressure of  $P_c = 345$  kPa (50 psia), and temperatures of  $T_c = 2220$ , 2780, and 3390 K (4000, 5000, and 6100°R, respectively) were simulated. The first value is considered the lower end of acceptable flight system performance, while the latter value is the maximum allowable temperature because of absorber material limitations.<sup>1</sup> One simulation with  $T_c = 2780$  K and  $P_c = 173$  kPa (25 psia) was also made to study the performance impact of pressure losses in the propellant feed system. A smaller, representative set of hydrogen recombination rates was chosen for the numerical study. These rates are summarized in Table 1 in terms of the constants for the Arrhenius rate form of Eq. (2). The Wetzell and Solomon high rate set<sup>4</sup> represents the fastest hydrogen re-

Table 1  $H_2$  recombination rate constants<sup>a</sup>

Reference	$M_i$	$A_i$	$N_i$	$E_{ci}/R$
4	$H_2$	$2.0 \times 10^{10}$	0	0
	H	$6.0 \times 10^{10}$	0	0
6	$H_2$	$2.98 \times 10^{10}$	-0.45	-755.3
	H	$9.43 \times 10^{10}$	-0.34	604.2
8	$H_2$	$5.0 \times 10^9$	0	0
	H	$5.0 \times 10^9$	0	0
5	$H_2$	$1.83 \times 10^{12}$	-1.0	0
	H	$7.3 \times 10^{11}$	-1.0	0

<sup>a</sup>Eq. (2),  $k_i$  in units of  $m^6/kmol^2 \cdot s$ .

Table 2 Predicted performance for  $T_c = 3390$  K,  $P_c = 345$  kPa

Rate	$F$ , N	$\dot{m}$ , kg/s	$I_{sp}$ , s	$\eta$	$Re^*$
Frozen	4.328	$4.37 \times 10^{-4}$	1009	0.966	4177
Ref. 5	4.328	$4.36 \times 10^{-4}$	1011	0.965	4168
Ref. 6	4.328	$4.35 \times 10^{-4}$	1015	0.958	4151
Ref. 8	4.333	$4.33 \times 10^{-4}$	1021	0.959	4129
Ref. 4	4.341	$4.26 \times 10^{-4}$	1038	0.948	4068
Equilibrium	4.697	$4.18 \times 10^{-4}$	1145	0.932	3990

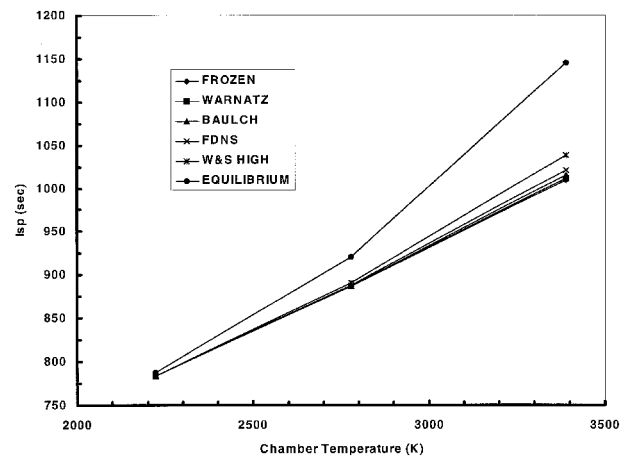


Fig. 3 Solar thermal rocket  $I_{sp}$  vs temperature,  $P_c = 345$  kPa.

combination rates found in the literature. The Baulch<sup>6</sup> and FDNS<sup>8</sup> rate sets produce moderate rates. The Warnatz<sup>5</sup> rate set generally characterizes the slowest rates. Reverse dissociation reaction rates are determined by the law of mass action. Nozzle chemistry was also modeled by the two extremes of frozen and equilibrium. The  $I_{sp}$  variation with chamber temperature for the various kinetic rates at a chamber pressure of 345 kPa is shown in Fig. 3.

At the highest temperature and nominal pressure ( $T_c = 3390$  K,  $P_c = 345$  kPa, respectively) approximately 12% of the hydrogen mass is dissociated in the plenum. With equilibrium chemistry, hydrogen completely recombines in the core flow just downstream of the throat, but a significant level of dissociation is maintained near the hot nozzle wall. All of the finite rate kinetics models produce nearly frozen chemistry throughout the short nozzle.

Table 2 shows the predicted values for thrust  $F$ , mass flow rate  $\dot{m}$ , and specific impulse  $I_{sp}$ . Increasing the kinetic rate increases the thrust and decreases the mass flow rate because of a decrease in the gas density. Depending on whether fast or slow kinetics are used, the maximum deviation in predicted  $I_{sp}$  is  $\pm 13.5$  s, or 1.3% of the mean specific impulse of 1024.5 s. Finite rate chemistry reduces the  $I_{sp}$  an average of 120.5 s from the ideal chemical equilibrium value.

Also shown in Table 2 are the nozzle  $I_{sp}$  efficiency and throat

Reynolds number.<sup>11</sup> The  $I_{sp}$  efficiency is the ratio of the actual  $I_{sp}$  to the inviscid  $I_{sp}$

$$\eta = \frac{I_{sp,actual}}{I_{sp,ideal}} \quad (4)$$

and is thus a measure of viscous losses. Inviscid  $I_{sp}$  values were calculated with the TDK code.<sup>9</sup> The nozzle throat Reynolds number is defined as

$$Re^* = 2\dot{m}/\pi r^* \mu_c \quad (5)$$

where  $r^*$  is the nozzle throat radius, and  $\mu_c$  is the chamber viscosity. For a generally constant pressure in the nozzle throat, faster kinetics produce higher temperatures and lower densities. The Reynolds number and  $\eta$  values decrease as density decreases, indicating increasing boundary-layer thickness and viscous losses. Table 2 shows that the net  $I_{sp}$  actually increases with increasing kinetic rate. These opposite trends indicate that kinetic losses are the dominant loss mechanism. Increasing the recombination rate reduces the kinetic losses, but increases the nozzle viscous losses, thus moderating the  $I_{sp}$  improvement.

Because of the low initial degree of dissociation, the uncertainty in kinetic rate only produced a 0.2%  $I_{sp}$  uncertainty with  $T_c = 2780$  K and  $P_c = 345$  kPa. At the lowest chamber temperature (2220 K), the  $I_{sp}$  uncertainty caused by the kinetic rate is negligible. Halving the chamber pressure from 345 to 173 kPa at 2780 K halved the thrust and mass flow rate, slightly decreased the  $I_{sp}$ , and produced a 0.2%  $I_{sp}$  uncertainty. Therefore, chamber pressure has only a slight impact on the influence of hydrogen kinetic rate uncertainty.

Based on this investigation and the recommendations of other researchers, the Baulch et al.<sup>6</sup> kinetic rates are recommended as nominal rates for future numerical predictions of solar thermal rocket performance.

### Acknowledgment

CFD Research Corporation provided the CFD-ACE™ code under an educational licensing agreement.

### References

- <sup>1</sup>Shoji, J., "Solar Thermal Propulsion Transfer Stage (STPTS)," Rockwell International, Rocketdyne Div. Briefing Presentation, Canoga Park, CA, 1993.
- <sup>2</sup>O'Leary, R. A., and Beck, J. E., "Nozzle Design," *Threshold*, Rockwell International, Rocketdyne Div., No. 8, 1992, pp. 34–43.
- <sup>3</sup>Gerrish, H. P., Jr., and Doughty, G. E., "Performance Assessment of Low Pressure Nuclear Thermal Propulsion," NASA TM-108433, Dec. 1993.
- <sup>4</sup>Wetzel, K., and Solomon, W., "Hydrogen Recombination Kinetics and Nuclear Thermal Rocket Performance Prediction," *Journal of Propulsion and Power*, Vol. 10, No. 4, 1994, pp. 492–500.
- <sup>5</sup>Oldenberg, R., "Hypersonic Combustion Kinetics—Status Report of the Rate Constant Committee, NASP High-Speed Propulsion Technology Team," NASP TM 1107, May 1990.
- <sup>6</sup>Baulch, D. L., Drysdale, D. D., Horne, D. G., and Lloyd, A. C., *Evaluated Kinetic Data for High Temperature Reactions*, Vol. 1, Butterworths, London, 1972, pp. 261–326.
- <sup>7</sup>Cohen, N., and Westberg, K. R., "Chemical Kinetic Data Sheets for High-Temperature Chemical Reactions," *Journal of Physical Chemistry Reference Data*, Vol. 12, No. 3, 1983, pp. 531–590.
- <sup>8</sup>Chen, Y. S., "FDNS, A General Purpose CFD Code, User's Guide, Version 3," Engineering Sciences, Inc. TR-93-01, May 1993.
- <sup>9</sup>Nickerson, G. R., Berker, D. R., Coats, D. E., and Dunn, S. S., "Two Dimensional Kinetics (TDK) Nozzle Performance Computer Program," Vols. I–III, NASA8-39048, 1993.
- <sup>10</sup>CFD-ACE™, version 1.6: *Theory Manual*, CFD Research Corp., Huntsville, AL, March 1993.
- <sup>11</sup>Grisnik, S. P., Smith, T. A., and Saltz, L. E., "Experimental Study of Low Reynolds Number Nozzles," NASA TM-89858, May 1987; also AIAA Paper 87-0992, May 1987.

## Off-Design Performance Prediction of Single-Spool Turbojets Using Gasdynamics

Mirza F. Baig\*

Aligarh Muslim University, Aligarh 202001, India  
and

H. I. H. Saravanamuttoo†

Carleton University,  
Ottawa, Ontario K1S 5B6, Canada

### Nomenclature

$A$	= area of exhaust nozzle
$C_p$	= specific heat at constant pressure
$M$	= Mach number
$\dot{m}$	= mass flow
$N$	= engine mechanical speed
$P$	= pressure
$R$	= gas constant
$T$	= temperature
$\epsilon_c$	= compressor pressure ratio
$\eta_c$	= polytropic compressor efficiency
$\eta_m$	= mechanical efficiency
$\eta_t$	= polytropic turbine efficiency
$\psi$	= $T_{t4}/T_{t2}/(T_{t4}/T_{t2})_{des}$

### Subscripts

$a$	= air
des	= design
$t$	= total
0	= ambient atmosphere

### I. Introduction

OFF-DESIGN performance of aeroengines is of major interest, not only to the user, but also the manufacturer, as the analysis can be of use for preliminary performance calculations for parametric studies, particularly for aircraft design purposes.

Mattingly et al.<sup>1</sup> developed a code that did not need the use of performance maps, but it gave results having more than 10–15% error in fuel flow and thrust, even at cruise flight conditions. Wittenberg<sup>2</sup> devised an approach based on gasdynamic relationships, making the use of compressor and turbine maps redundant. The present work is a modified extension of Wittenberg's approach,<sup>2</sup> as it tries to compute overall engine performance by ascertaining turbine entry temperature (TET), knowing just the flight conditions and the corrected engine speed.

### II. Off-Design Analysis

The design point analysis of a single-spool turbojet can usually be done by thermodynamic component-to-component analysis, starting with a diffuser, compressor, combustor, turbine, and a propelling nozzle. It is straightforward and can be found in text, such as *Gas Turbine Theory*.<sup>3</sup> Figure 1 shows a schematic view of a single-spool turbojet with station numbering.

The off-design analysis revolves around two conditions: 1) when the aircraft is idling or descending (in both cases the

Received May 10, 1996; revision received April 28, 1997; accepted for publication May 8, 1997. Copyright © 1997 by the American Institute of Aeronautics and Astronautics, Inc. All rights reserved.

\*Lecturer, Department of Mechanical Engineering. Member AIAA.  
†Professor, Department of Mechanical and Aerospace Engineering. Associate Fellow AIAA.